Journal of Structural Geology, Vol. 11, No. 1/2, pp. 147 to 162, 1989
Printed in Great Britain

0191-8141/89 $03.00 + 0.00

Coupled grain-scale dilatancy and mass transfer during deformation at high fluid pressures: examples from Mount Lyell, Tasmania

S. F. Cox

Research School of Earth Sciences, The Australian National University, G.P.O. Box 4, Canberra, A.C.T., 2601, Australia

and

M. A. Etheridge

Bureau of Mineral Resources, Geology and Geophysics, G.P.O. Box 378, Canberra, A.C.T. 2601, Australia

(*Received* 16 *June* 1988; *accepted* 2 *September* 1988)

Abstract—High fluid pressures have promoted the coupled operation of grain-scale dilatancy and solution–precipitation processes as dominant deformation mechanisms during cleavage development in a sequence of Cambrian silicic volcanics in the Mount Lyell area, Tasmania. Episodic opening of pervasive microcracks has localized the precipitation of material removed from dissolution sites, and has led to the growth of oriented crack–seal microstructures which are a major element of the overall deformation microfabric. It is argued that transient, dilatancy-driven fluid pressure gradients, and consequent fluid migration within the fluid-containing grain-boundary and microcrack network, can play an important role in contributing to mass transfer between dissolution sites and dilatant microfracture sites.

The enhancement of grain-scale microfracture processes and coupled solution–precipitation processes, which accompanies the development of near-lithostatic fluid pressures, is expected to lead to high fluid pressure crustal regimes becoming substantially weaker than otherwise similar low fluid pressure regimes. The onset of such weakening processes in response to rising fluid pressures is probably a significant factor triggering pervasive regional deformation of the upper-crust.

INTRODUCTION

In low-grade metamorphic terranes, deformation processes are usually controlled by aqueous fluid transport mechanisms operating in conjunction with dissolution and precipitation processes (e.g. Durney 1972, Nickelsen 1972, Williams 1972a, Means 1977a, Borradaile *et al.* 1982, Rutter 1983, Etheridge *et al.* 1984, Cox *et al.* 1987). Shortening during deformation involving dissolution, solution-transfer and precipitation (i.e. pressure solution or solution–precipitation creep) is usually achieved by mass loss from grain surfaces or discrete zones which are oriented at high angles to the shortening direction (Borradaile *et al.* 1982). Precipitation of material removed from dissolution sites occurs in a variety of sites including pore spaces, pressure shadows, microfractures and vein arrays (Durney 1972, 1976, Williams 1972b, Beach 1974, Means 1975, Ramsay 1980, Cox & Etheridge 1983, Cox *et al.* 1987). Material transfer between dissolution sites and precipitation sites has in many cases been ascribed to diffusional processes (Durney 1972, 1976, Kerrich 1978, Rutter 1983). However, deformation can involve significant local mass loss and consequent long-range mass transport (Alvarez *et al.* 1978, Geiser & Sansone 1981, Wright & Platt 1982, Gratier 1983, Beutner & Charles 1985), requiring that mass transfer via a migrating fluid phase plays an important role in many low-grade metamorphic terranes (Engelder 1984, Etheridge *et al.* 1984, Green 1984).

The importance of high fluid pressures in enhancing permeability and promoting fluid migration and mass transfer during crustal deformation has been emphasized by Etheridge *et al.* (1984) and Cox *et al.* (1987). This paper describes and discusses some spectacular examples in which permeability has been enhanced by grain-scale dilatancy during regional deformation of a sequence of low-grade metamorphosed silicic volcanic rocks. In these examples, dissolution and mass transfer during cleavage development have been coupled with precipitation of material in a network of episodically dilatant grain-scale microfractures. We wish to highlight the importance of high fluid pressures in promoting *pervasive* dilatancy during cleavage development, and demonstrate that the development of oriented microstructures within dilating microcracks, as well as in dissolution sites, can play a particularly important role in the development of deformation microfabrics. We also explore the implications of episodic grain-scale dilatancy for mass transfer processes during rock deformation, and examine the consequences that high fluid pressures and coupling of dilatancy and solution transfer may have for upper crustal strength during regional deformation.

GEOLOGICAL SETTING

The deformed volcanic rocks which are the subject of this paper occur within the Cambrian Mount Read Volcanics of western Tasmania (Corbett 1981). This region lies within the southern portion of the Palaeozoic Lachlan Fold Belt of eastern Australia (Williams 1978).

The volcanic sequence in the Mount Lyell area contains over 4000 m of silicic pyroclastics and lavas, together with less common intermediate volcanics, and minor intercalated sediments. Extensive but varied hydrothermal alteration of parts of the sequence was associated with syngenetic base metal mineralization (Reid 1975).

Regional Middle Devonian deformation at low metamorphic grade has produced two orientational groups of folds in the area (Cox 1981). First generation (D_1) folds are large-scale, upright and tight structures which control the gross bedding geometry and have NNW-trending axial surfaces. A first generation axial surface cleavage shows only sporadic weak development in the area. Open W- to WNW-trending upright second generation (D_2) folds are prominent in the well-layered sedimentary sequences overlying the volcanic sequence, but are not well-developed in the poorly stratified volcanic sequence itself. D_2 strain in the volcanic sequence has been accommodated largely by the development of a mesoscopically penetrative upright foliation (S_2) which is essentially axial planar to D_2 folds in the overlying sedimentary sequence. An associated steeply plunging mineral elongation lineation (L_2) is well developed on S_2. The D_2 deformation fabrics, which are the subject of this paper, have developed in response to approximately plane strain deformation involving shortenings typically in the range 30–60% perpendicular to S_2 and elongations typically ranging from about 50–150% parallel to L_2 (Cox 1981).

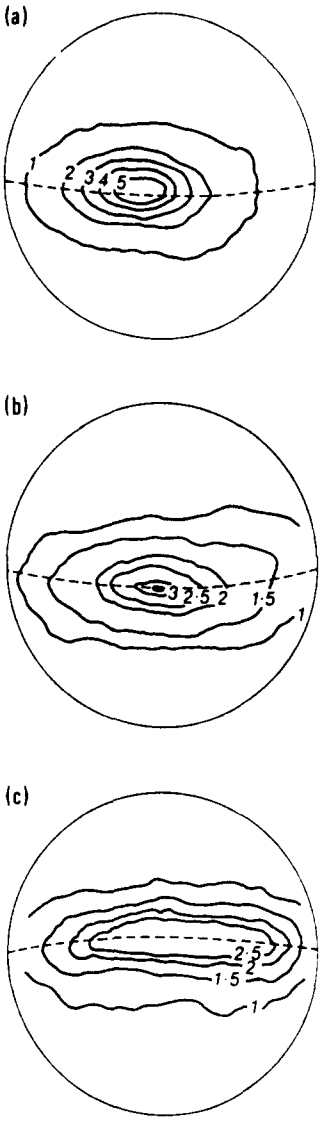

Fig. 1. Typical layer silicate (002) preferred orientations in deformed silicic volcanics from the Mount Lyell area. Contour intervals are x-uniform. S_2 is perpendicular to the (002) pole maximum; L_2 is the pole to the (002) partial girdle. The pole figures for both phengite and chlorite have a nearly orthorhombic symmetry. (a) Chlorite (002). (b) Phengite (002). (c) Chlorite (002).

MICROFABRICS—GENERAL ASPECTS

At the grain-scale, the S_2/L_2 deformation fabric in the volcanic sequence is defined by a number of microfabric elements. These include (001) and shape preferred orientations in layer silicates (Fig. 1), shape preferred orientations of other phases, and fabric discontinuities such as layer silicate films and related domainal structures (Figs. 2–5). The main processes whereby original microstructures have been modified during deformation are *dissolution* and *microfracturing*. The development of new microfabric elements during deformation has been dominated by the development of layer silicate films at *dissolution sites*, and by the growth of oriented fibrous microstructures at *microfracture sites* within the interfilm domains. Descriptions of the microfabrics in these two types of sites are presented in the following sections.

MICROFABRICS AT DISSOLUTION SITES: LAYER SILICATE FILMS AND RELATED STRUCTURES

Oriented layer silicate films, film clusters or bundles, and related domainal concentrations of phases such as fine-grained rutile and magnetite are well-developed in the volcanic sequence (Figs. 2 and 3) and exhibit characteristics similar to those described in many deformed low-grade metasedimentary sequences (e.g. Means 1975, Gregg 1985, Southwick 1987). Layer silicate films typically occur as thin, subplanar to anastomosing sheets of layer silicates which are subparallel to the mesoscopic S_2 orientation, and contain layer silicate grains having (001) dominantly subparallel to the film length (Figs. 2 a & b). The anastomosing habit of films, particularly around coarse quartz and feldspar grains or grain aggregates leads to a scatter of (001) poles around the mean S_2 orientation. In many cases, films are more strongly anastomosing in sections normal to L_2 (N-sections) than in sections perpendicular to S_2 and parallel to L_2 (P-sections). This contributes to a larger spread of (001) poles about a girdle normal to L_2 than about the direction normal to this, and is a key factor in defining the linear component of the fabric (Fig. 1).

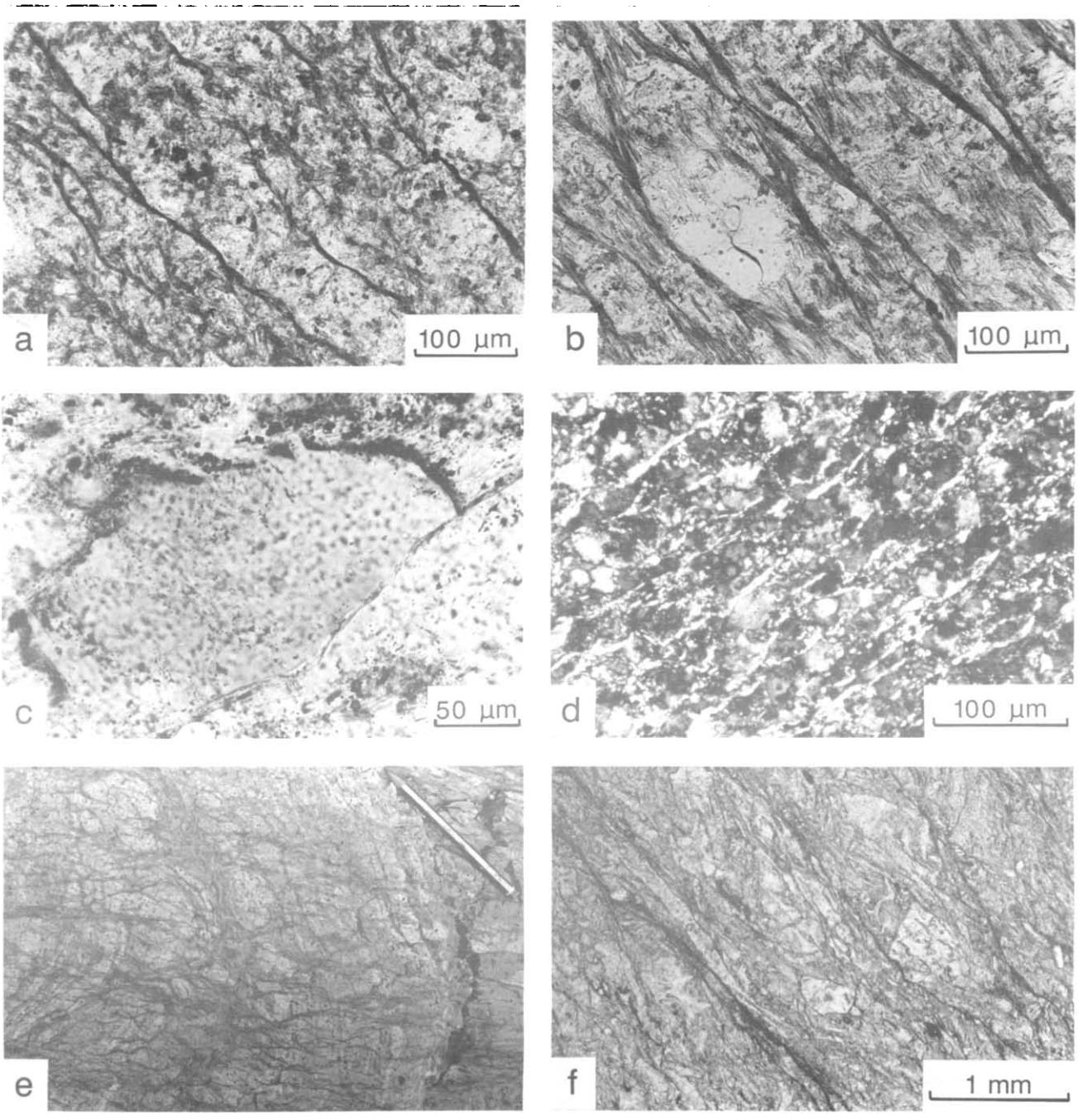

Fig. 2. Layer silicate films and associated structures in volcanics. (a) N-section (normal to L_2) of hydrothermally altered silicic tuff. Sinuous to anastomosing chlorite films are subparallel to the mesoscopic S_2 foliation and have (001) subparallel to the film length. Very little layer silicate preferred orientation is apparent in the interfilm domains in this section (plane polarized light, PPL). (b) P-section (parallel to L_2) of the rock depicted in (a). Note the strong layer silicate (001) and grain shape preferred orientation in the interfilm domains (PPL). (c) Truncation of quartz grain due to dissolution at the site of a layer silicate film (PPL). (d) Short layer silicate films in a layer-silicate-poor silicic volcanic (N-section, cross-polarized light, XPL). (e) Anastomosing discontinuous layer-silicate-enriched domains cutting across flow banding in outcrop P-section of a hydrothermally altered rhyolite. (f) Vitric tuff with opaque mineral enriched domains coincident with layer silicate films (PPL).

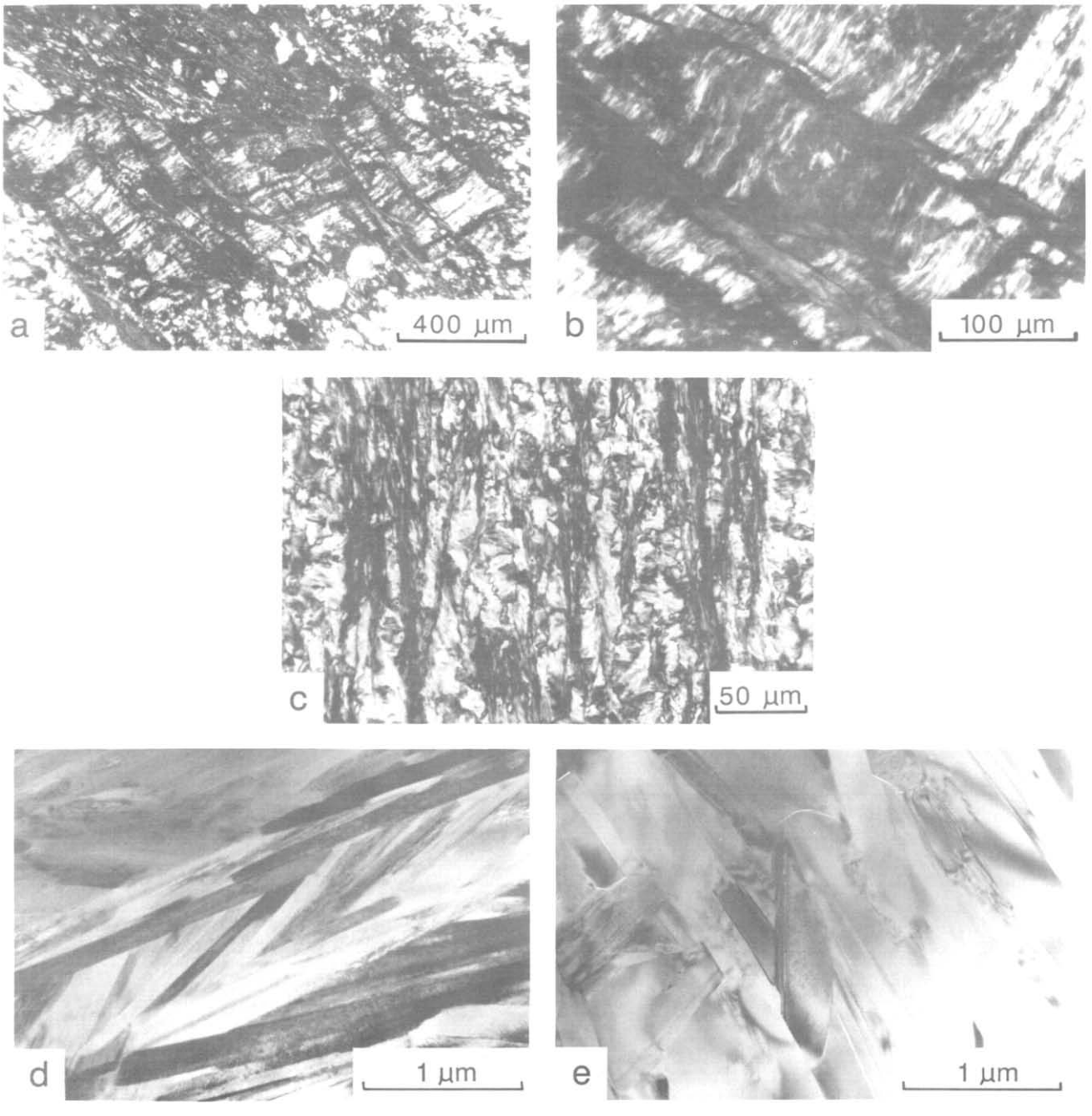

Fig. 3. Layer silicate films in layer-silicate-rich assemblages. (a) Chlorite films developed within a chlorite pseudomorph after a biotite phenocryst in a hydrothermally altered crystal–vitric tuff (PPL). (b) Detail of chlorite films in (a) (PPL). (c) Domainal layer silicate film development in a pure layer silicate aggregate (XPL). (d) Transmission electron micrograph showing detail of oriented layer silicate microstructure illustrated in (c). Small domains of undeformed mica are inclined to more elongate, foliation-defining micas. (e) Elongate foliation-parallel micas intergrown with shorter micas inclined to the foliation (TEM).

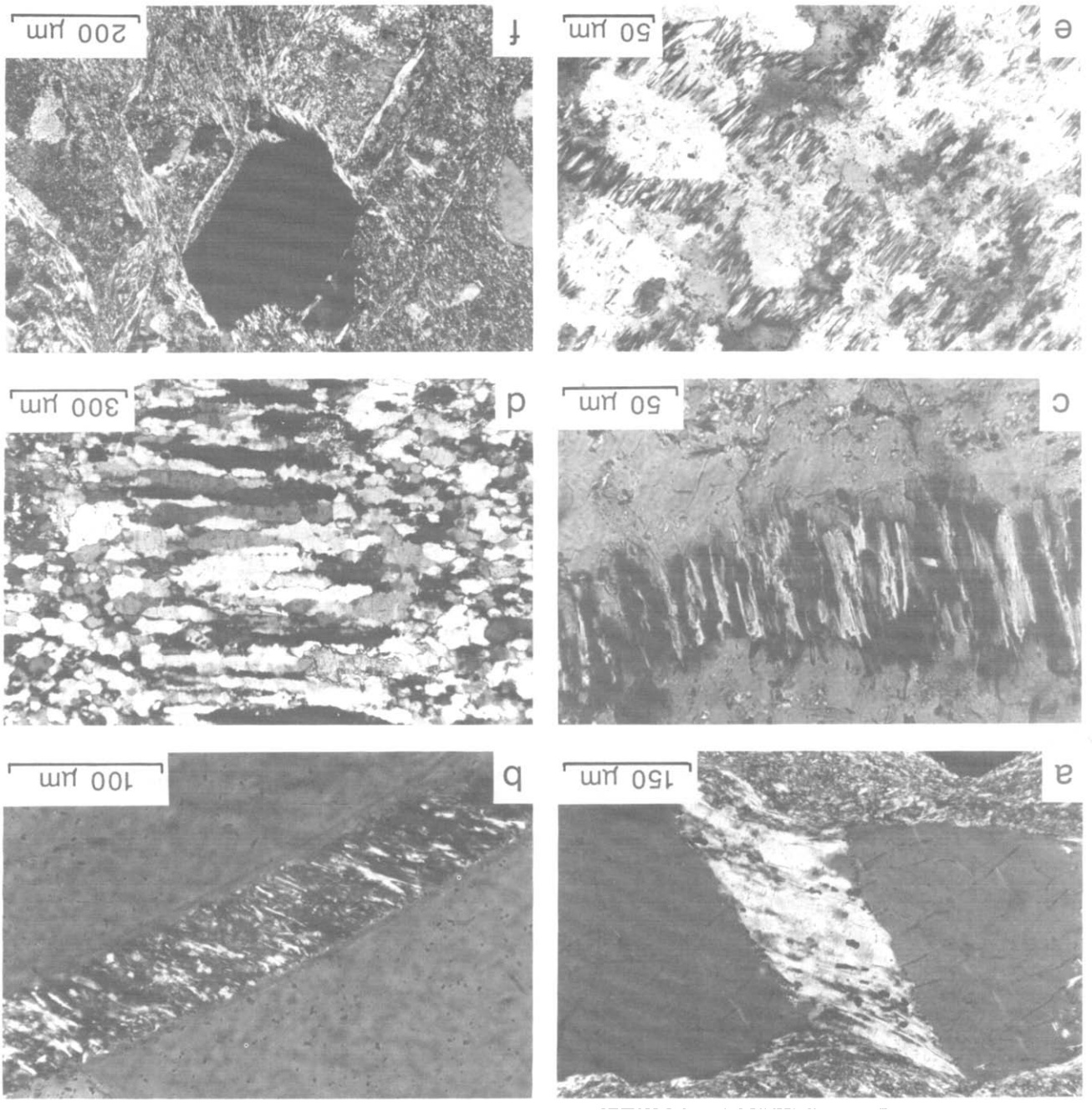

Fig. 4. Fibrous microstructures in deformed silicic volcanics. (a) Intragranular microfracture in a quartz phenocryst. The microfracture site has been sealed by fibrous quartz and mica having fibre long axes approximately parallel to the extension direction across the microfracture. The microfracture apparently has not propagated into the adjacent finer grained matrix. Note the zone of inclusions along the original microfracture walls on the quartz phenocryst (XPL). (b) Oriented intergrowth of mica and quartz in an oblique extension microfracture within a quartz phenocryst. Note the syntaxial overgrowth rims of quartz against the original microcrack walls, and also the presence of some irregularly oriented mica grains amongst the highly oriented ones (XPL). (c) Intergrowth of fibrous albite and mica in an intragranular extension microfracture site in a feldspar phenocryst (XPL). (d) Fibrous microvein in hydrothermally altered volcanic. Individual quartz fibres are usually syntaxial overgrowths of grains in the vein wall (XPL). (e) Fibrous intergrowth of quartz and layer silicates in a transgranular extension site in a hydrothermally altered volcanic (XPL). (f) Conjugate sets of oblique extension microfractures forming a lozenge pattern. The microfracture sites contain fibrous mica with (001) acutely inclined to microfracture walls (see text for description) (XPL).

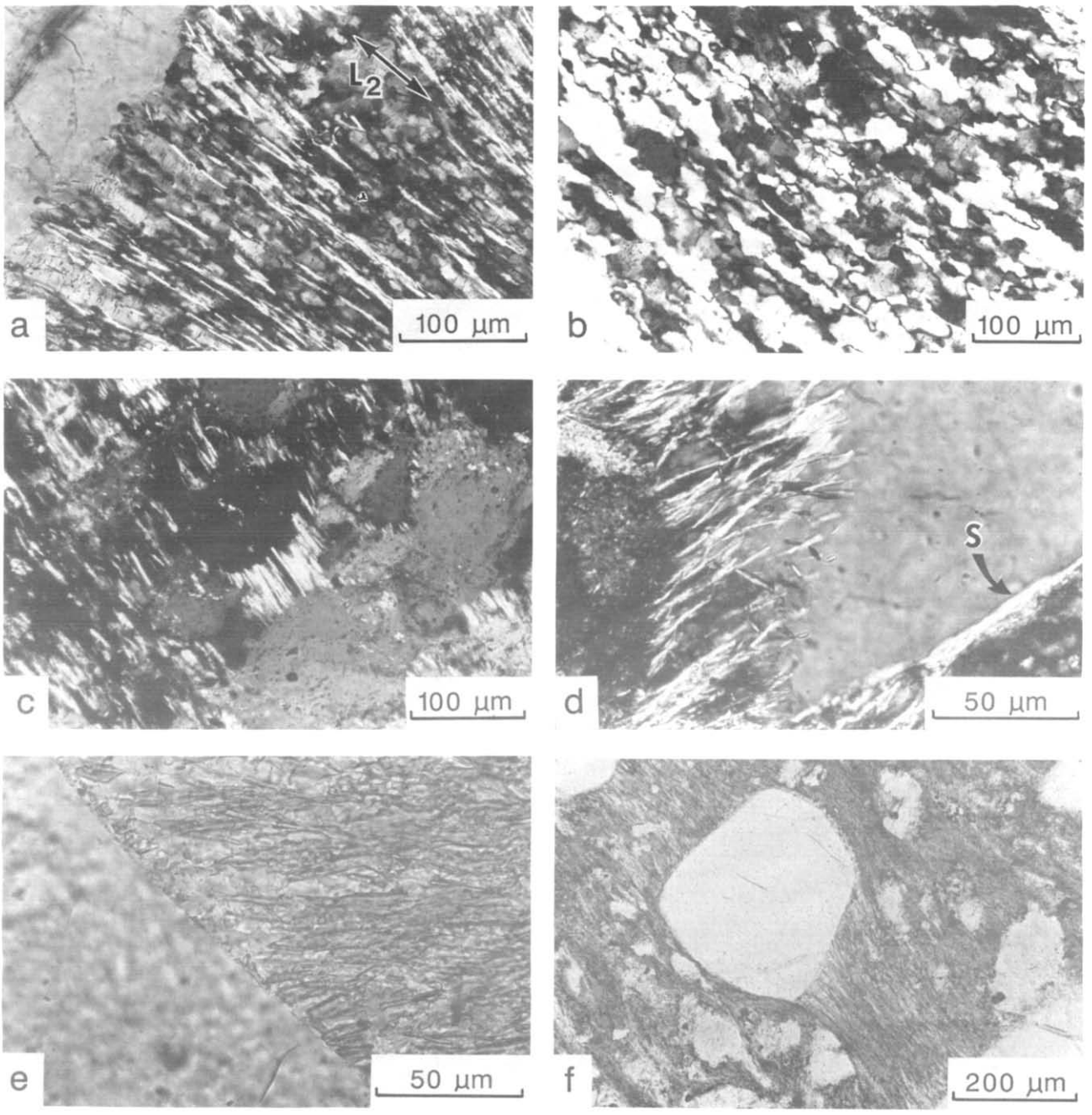

Fig. 5. Fibrous intergranular microstructures in deformed silicic volcanics. (a) Oriented fibrous quartz–mica intergrowth developed adjacent to a quartz phenocryst grain surface which is inclined at a high angle to L_2 (XPL). (b) Fibrous quartz microstructure developed in a fine-grained, originally equant microstructure in a siliceous rock produced by intense hydrothermal alteration of a silicic volcanic (XPL). (c) Intergranular fibrous quartz–mica intergrowth in a hydrothermally altered silicic volcanic (XPL). (d) Fibrous mica–quartz intergrowth on the end of a quartz phenocryst where its grain surface is at a high angle to L_2. Note development of irregularly oriented mica platelets in parts of the syntaxial overgrowth rim, and evidence for solution of quartz and development of a layer silicate film (marked S) where quartz grain surface is at a low angle to S_2. (e) Fibrous intergrowth of chlorite and quartz forming part of a beard on the end of a quartz phenocryst. Misoriented layer silicates are present at the phenocryst grain surface. Note the sharply defined phenocryst boundary (PPL). (f) Cuspate beard microstructure extending between two quartz phenocrysts (PPL).

Layer silicate films form major fabric discontinuities against which various primary volcanic and clastic microfabric elements are truncated (Figs. 2c and 3a). Such features indicate that significant dissolution and mass loss has occurred at layer silicate film sites.

The extent of development of layer silicate films in the volcanics depends on both rock composition and strain. For example, fine-grained devitrified lavas which have only minor hydrothermal alteration, and consequently only a small proportion (<10% by volume) of layer silicates, have only a weakly developed mesoscopic foliation which is expressed microscopically by the presence of short layer silicate films (Fig. 2d). Individual layer silicate grains within films are usually less than 4 μm wide, and up to about 15 μm long parallel to (001). With increasing whole-rock layer silicate content film development becomes more pronounced. In many volcanics, whose groundmass contains around 15–30% layer silicates, films are separated by interfilm domains which are seldom more than about 100 μm wide. Quartz and feldspar grains which are bounded by films are typically elongate parallel to the films due to dissolution at interfaces abutting films.

Layer silicate films usually have an inhomogeneous distribution. For example, in areas inferred to have relatively high strain, such as areas of fine groundmass adjacent to large undeformed phenocrysts where their grain surfaces are at low angles to S_2, films are longer and more closely spaced than in adjacent lower strain regions. In strain shadows adjacent to phenocryst grain surfaces which are inclined at high angles to S_2, films are commonly not present or are very rudimentary.

Layer silicate films can also occur in closely spaced clusters which give rise to a mesoscopic differentiated layering (Fig. 2e). Such clusters form foliation-parallel, layer silicate-rich domains which are up to about 1 mm wide and extend for several tens of centimetres. The film-poor domains between the film cluster domains can be up to several centimetres wide. Partly dissolved relict quartz or feldspar grains, phenocrysts and devitrification microspherulites caught up in film clusters are markedly elongate parallel to the domain boundary. However, there is no evidence for intracrystalline deformation of quartz or feldspar.

Observations on spacing, width, and length of layer silicate films suggest that with increasing strain, films become longer and thicker, as well as becoming more closely spaced. Their development has involved dissolution and removal of material at boundaries between films and interfilm domains, together with formation of oriented layer silicates at these sites. The dissolution and removal of quartz, feldspars and carbonate, and the concentration of layer silicates and other phases such as rutile at dissolution surfaces (Fig. 2f) points to the preferential removal of Si, Na and Ca from these sites, with consequent increase of local K, Fe, Mg, Al and Ti concentrations.

The microstructure of layer silicate films in pure layer silicate aggregates in strongly hydrothermally altered volcanics provides important insights into the processes involved in film generation. In the example illustrated in Figs. 3 (a) & (b), chlorite having (001) at a high angle to S_2 has pseudomorphed an original biotite phenocryst in a silicic tuff, probably during pre-deformation hydrothermal alteration. In several places the (001) cleavage trace has been gently crenulated subparallel to the external S_2 orientation. Chlorite films have developed along some of these crenulated zones, whereas other films are apparently unrelated to crenulations. Individual films consist of elongate chlorite grains, each up to 10 μm wide and up to about 50 μm long, with (001) and grain long dimensions subparallel to the film length. Where the films propagate into the surrounding groundmass, stepping of the boundaries of the pseudomorphs across films is consistent with shortening by mass loss from the film sites.

Microprobe analyses of host and film chlorites indicate that the film chlorite is richer in iron, though Si/Al and Si/Mg ratios are essentially the same in the two chlorite types (Fig. 6). The host chlorite is sharply truncated by the oriented film chlorite without any significant rotation of the former.

Domainal mica film development in a fine-grained, initially random mica aggregate produced by extreme hydrothermal alteration of a silicic volcanic is illustrated in Fig. 3(c). In this example the anastomosing mica films which define S_2 are up to 50 μm wide and extend up to 1 mm parallel to S_2. The grain elongation and (001) orientation in the films is dominantly subparallel to the film length. Individual platelets are usually less than 2 μm wide, but have lengths up to 20 μm parallel to (001). The micas in the interfilm domains occur as aggregates of irregularly oriented grains which are coarser than those in the film domains. In both the films and elongate interfilm domains the micas are typically undeformed. Again there is no evidence of rotation of layer silicates at film margins and the oriented film micas abruptly truncate the variably oriented and coarser-grained interfilm micas.

Transmission electron microscopy confirms that both film and interfilm layer silicates are usually undeformed (Fig. 3 d&e). Within films, individual layer silicate grains can be up to 20 μm long if they are oriented with (001) subparallel to the foliation. However grains with (001) inclined to the film length are present, but are much shorter parallel to (001). Grain boundaries are usually formed by the (001) plane of one of two adjacent grains.

The microstructures we have described provide constraints on the mechanisms by which the layer silicate films have developed. There is a general lack of evidence for substantial grain rotation, kinking, or significant dislocation creep in pre-deformation layer silicates at film boundaries. These factors, together with the abrupt truncation relationships and changes in grain size and composition between relict pre-deformation layer silicates and film-defining layer silicates, indicate that film generation has not involved rotation of pre-existing grains into the film plane. Instead, film development has involved ionic exchange reactions and oriented growth of new layer silicates in discrete domains from which a significant volume of material has been removed.

FIBROUS MICROFABRICS IN INTERFILM DOMAINS

In the interfilm domains a variety of pre-deformation microstructures is well preserved. These include phenocrysts, devitrified and hydrothermally altered microspherulites, shards, pumice clasts and lithic or crystal clasts. Where the opposing surfaces of such grains or grain aggregates are inclined at moderate to high angles to the L_2 direction, they are usually separated by domains containing fine-grained fibrous microstructures. In these sites the fibres are elongate in a direction subparallel to L_2.

Quartz and feldspar are usually abundant in the fibrous domains, but may be intergrown with a major proportion of fibrous to platy layer silicates, particularly in the more aluminous, hydrothermally altered volcanics. However, in some volcanics having a modal composition dominated by quartz and feldspar, layer silicates can still be dominant phases in both the film domains and the fibrous parts of the interfilm domains (e.g. Figs. 2b and 4c, e & f).

Layer silicates in the fibrous domains typically have a weak or nearly random (001)-trace orientation in N-sections (Fig. 2a), but appear as highly oriented fibres with long axes and (001)-traces subparallel to, or gently inclined to, L_2 in P-sections (Fig. 2b). Thus the layer silicate (001) orientation in the interfilm domains contributes in a major way to the spread of (001) poles normal to L_2 (Fig. 1). The volume fraction of sites having fibrous microstructures ranges from about 20–60% in typical deformed volcanics in the Mount Lyell area.

In a number of cases it can be demonstrated clearly that the fibrous microstructures in interfilm domains have developed in progressively opening microfractures. The best examples are provided by the microstructures within opened *intragranular* microfractures which cut across relatively coarse grains such as phenocrysts. Similar microstructures are also developed in microfractures which cut across or around many grains (these sites will be termed '*transgranular* microfractures'). The abundant development of identical fibrous microstructures around parts of the surfaces of various pre-deformation fabric elements indicates that opening of

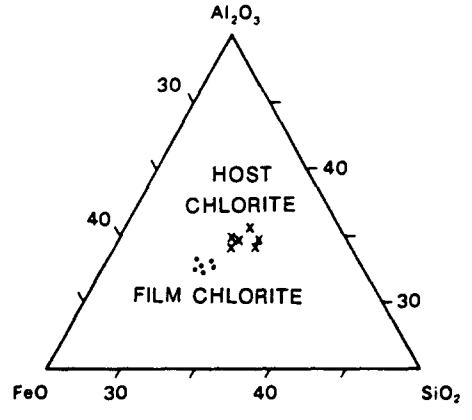

Fig. 6. Compositional variation between host and film chlorite depicted in Figs. 3 (a) & (b).

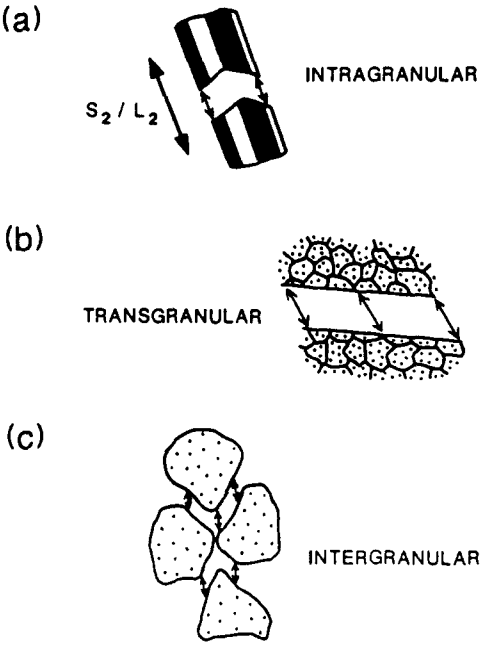

Fig. 7. Morphology of microfractures: (a) intragranular microfracture; (b) transgranular microfracture; (c) intergranular microfractures. Arrows indicate direction of opening.

intergranular microfractures has also been important during foliation development. The morphology of the major microfracture types is illustrated in Fig. 7.

Clearly recognizable microfractures range in type from pure extension microfractures, through oblique extension fractures (i.e. shear microfractures with a finite normal displacement) to less common compressive shear fractures or microfaults (Fig. 8). Transgranular shear or oblique extension fractures form conjugate sets which are symmetric about the S_2 foliation, with their intersection with the S_2 plane being approximately normal to L_2.

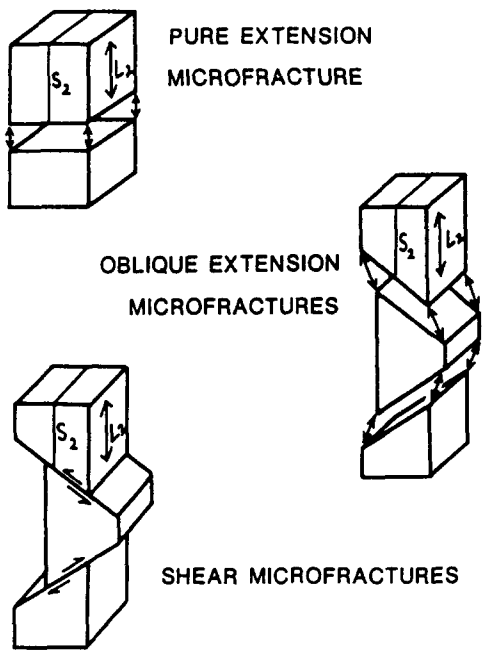

Fig. 8. Geometry of microfractures in relation to the S_2/L_2 fabric anisotropy.

The consistent orientation of extension microfractures at high-angles to the steeply plunging L_2 mineral elongation lineation indicates that at the time of fracture initiation the least principal stress (σ_3) was subparallel to L_2. The direction of opening across extension microfractures, as indicated by offsets of grain boundaries, twin boundaries and microfracture wall irregularities, is invariably subparallel to L_2. The sense of displacement across oblique extension and shear microfractures, where it can be judged by offsets of grain boundaries and other features, indicates shortening at high angles to S_2 and extension subparallel to L_2. Shear and oblique extension microfractures can be inclined to S_2 at angles as low as 30°.

In the following sections the fibrous microstructures developed in microfracture sites will be discussed in further detail.

Intragranular microfractures

The development of fibrous microstructures is particularly well illustrated within intragranular microfractures in quartz and feldspar phenocrysts, coarse-grained volcaniclastic fragments and devitrification microspherulites (Fig. 4).

Intragranular microfractures have planar to irregular shapes, and have openings up to about 100 μm. Opening of microfractures in phenocrysts seldom has resulted in more than 50% local elongation subparallel to the L_2 direction. Intragranular microfractures within phenocrysts usually do not propagate into the adjacent groundmass (Fig. 4a).

Narrow ($\leq$30 μm) microfractures can be filled by a syntaxial overgrowth on the host grain. In quartz phenocrysts, for example, overgrowths can be distinguished from the host grain by having a different incidence, or type, of solid-phase inclusions, or be delineated by a surface rich in fine solid-phase or fluid inclusions (Fig. 4b). Where the opening across microfracture walls is greater than about 30 μm, or where a syntaxial overgrowth rim is not present, microfracture sites are usually occupied by spectacular fibrous microstructures. Quartz and feldspar fibres have cross-sectional diameters of 10–30 μm, and long axes subparallel to the opening direction across the separated microfracture walls, regardless of the orientation of the microfracture wall. These fibres can contain transverse fluid-inclusion-rich surfaces which are subperpendicular to fibre long axes and spaced at irregular intervals up to 20 μm apart. These are interpreted as incompletely sealed intrafibre microfracture sites (Simmons & Richter 1976) and indicate that fibre growth has occurred by a crack–seal mechanism involving repeated microcracking and sealing by syntaxial overgrowth. Such fibrous microstructures are similar to 'stretched-crystal' fibres in veins (Durney & Ramsay 1973). The fact that fibres connect originally joined positions on either side of intragranular microfractures, and that they are commonly non-perpendicular to the initial microfracture walls is consistent with a crack–seal fibre growth mechanism which has tracked a displacement path (Cox & Etheridge 1983).

In layer silicate-rich volcanics, fibrous quartz or feldspar is usually intergrown with oriented layer silicates within intragranular microfracture sites (Figs. 4b & c). The layer silicate fibres and platelets are seldom greater than about 5 μm thick perpendicular to (001), and have their long axis in the (001) plane and usually subparallel to the opening direction across microfractures. Individual layer silicate fibres can extend across the full width of an intragranular extension microfracture site and attain lengths up to about 100 μm, but commonly they extend only part of the way across such sites. In many examples only layer silicate fibres having (001) and grain long axes subparallel to the extension direction are present. However, in other cases, small misoriented layer silicate grains are present adjacent to the initial microfracture walls, or are scattered amongst well oriented layer silicates within the main part of microfracture sites. The layer silicate fibres have no apparent orientation relationship with either the crystallographic orientation of the host grain or the orientation of the initial microfracture walls.

Cox & Etheridge (1983) have argued that the fibrous microstructures and layer silicate (001) preferred orientation in such intragranular microfracture sites have developed by crack–seal mechanisms involving repeated intrafibre crack–seal increments. The preferred orientation is considered to develop in response to preferential rejoining, by syntaxial overgrowth, of pulled apart layer silicate grains which have their fast growth directions parallel to the incremental displacement direction across a microcrack.

Transgranular microfractures

Fibrous microstructures identical to those developed in intragranular extension microfractures are present in transgranular microfractures which are oriented at high angles to the L_2 direction.

In quartz-rich hydrothermally altered volcanics, transgranular extension microfractures less than about 40 μm wide usually extend for up to several hundred microns at high angles to S_2. The fibrous quartz within them is usually a 'stretched-crystal' type of syntaxial overgrowth on quartz grains in the microcrack walls (Fig. 4d). Some wider transgranular extension microfractures exhibit microstructures indicative of syntaxial, antitaxial, 'stretched-crystal', or composite growth mechanisms (see Ramsay & Huber 1983, p. 241), and are transitional to abundant mesoscopically developed fibrous extension veins. Such veins and microveins can contain inclusion trails, inclusion bands, fibre–fibre serrations, and stepped albite twin lamellae indicative of growth by crack–seal mechanisms (Ramsay 1980, Cox & Etheridge 1983).

Offsets of matching microfracture wall irregularities indicate that, as in intragranular fibre sites, fibre long axes connect originally joined parts of microfracture

walls (Fig. 4e). Particularly in narrow microveins, quartz fibres clearly connect the pulled apart segments of originally joined grains.

Transgranular shear or oblique extension microfractures having a major component of displacement at low angles to the microfracture walls are symmetrically inclined about S_2 and L_2 (Figs. 4f and 8). Opening angles between apparently conjugate sets of such microfaults, or zones of grain translation, are typically in the range 50–90°, with L_2 being the acute bisectrix. In the crystal–lithic tuff illustrated in Fig 4(f), the distribution of dilatant shear microfractures containing fibrous mica has been controlled by boundaries between clasts. Quartz and layer silicate fibre long axes within dilatant shear microfractures lie in the acute angle between L_2 and the P-section trace of the microfracture boundary. This is consistent with fibre long axes being subparallel to the displacement direction, as is the case in extension microfractures. Similar zones of grain translation have been described in experimentally deformed aggregates (Means 1977b) and discussed by Borradaile (1981).

Intergranular microfractures

Intergranular 'stretched-crystal' quartz and feldspar and associated fibrous layer silicate microstructures are developed only on host-grain surfaces which are oriented at high to moderate angles to the L_2 direction (Fig. 5).

The development of fibrous quartz-dominated microstructures in intergranular sites can involve a history of repeated crack–seal growth near the host-grain surface, within the developing fibres, or adjacent to the boundary between the fibrous domain and the non-fibrous, fine-grained groundmass. An increase of fibre diameters towards host grain margins (Fig. 5a) may indicate that fibre growth occurred dominantly adjacent to the host grain. Alternatively, such changes in fibre diameter can be partly due to dissolution of fibres as they are progressively pulled away from stress shadows adjacent to host grains.

Very fine-grained, quartz-rich, hydrothermally altered volcanics show patchy development of 'stretched-crystal' fibrous quartz microstructures (Fig 5b). The distribution of fibres and fluid inclusion bands which are oriented at high angles to both L_2 and fibre long axes indicates fibre growth by repeated grain-scale microfracturing, pull-apart and syntaxial overgrowth of individual grains in the originally fine-grained equant microstructure which is still preserved in the least strained areas. With continued shortening the fibrous microstructures can be continually modified by dissolution–precipitation processes, thus enhancing the elongate grain fabric even further.

Oriented fine fibrous intergrowths of quartz and/or feldspar and layer silicates are spectacularly developed in the more layer silicate-rich rock types (Figs. 5c–f). These microstructures are similar to the layer silicate 'beard' microstructures which have been extensively documented in metasedimentary rocks (e.g. Williams 1972b, Means 1975, Gray 1978), and are identical to the fibrous intergrowths in the intragranular microfracture sites described earlier. Accordingly, fibrous structures present on the ends of grains, where their surfaces are inclined at high angles to L_2, are also interpreted to have developed by crack–seal processes. In cases where beard-like fibrous intergrowths extend all the way between grains (e.g. phenocrysts) which, prior to deformation must have been separated by fine groundmass (Fig. 5f), the development of the fibrous microstructure must have involved grain-scale intragranular and/or intergranular microfracture and fibre growth within the groundmass. The common hour-glass structure of beards is attributed to shortening of beards at high angles to S_2, as well as extension of the early-formed parts of the beards parallel to L_2 outside the strain shadows adjacent to the ends of large rigid host grains.

Fibrous fringe structures on pyrite euhedra

Within the intensely hydrothermally altered parts of the volcanic sequence, disseminated euhedral pyrite is abundant. Face-controlled fringe structures (Ramsay & Huber 1983, p. 268) composed of layer silicates and fibrous quartz are well developed on pyrite grains only where their surfaces are at moderate to high angles to L_2, and represent another clear example of growth of fibrous microstructures in extension sites during foliation development. The volume of fringe structures relative to that of the host pyrite grains varies enormously, but indicates local maximum principal extensions subparallel to L_2 ranging from less than 10% to in excess of 300% in extreme cases. The quartz fibres in fringes are typically undeformed, and straight to only gently curved. Partition surfaces separating differently oriented fibre aggregates on adjacent faces of pyrite euhedra are also subplanar in most instances, indicating a dominantly coaxial extension history during fibre growth (Ramsay & Huber 1983, Etchecopar & Malavieille 1987).

DISCUSSION

Relation between strain and microstructure

The deformation microstructures developed within the volcanic sequence in the Mount Lyell area highlight the importance that coupled grain-scale microcrack opening and solution–precipitation creep processes can have during deformation and foliation development. It is clear that foliation development has been controlled largely by the formation of *dissolution sites* (material sources) and dilatant *microfracture sites* (material sinks), and by the development of grain-shape and lattice preferred orientations in these two types of sites.

Strain has been accommodated largely by dissolution, microfracture and grain translation. The dissolution and removal of material from discrete surfaces along which layer silicate films develop by oriented growth mechanisms has led to local volume loss and has accom-

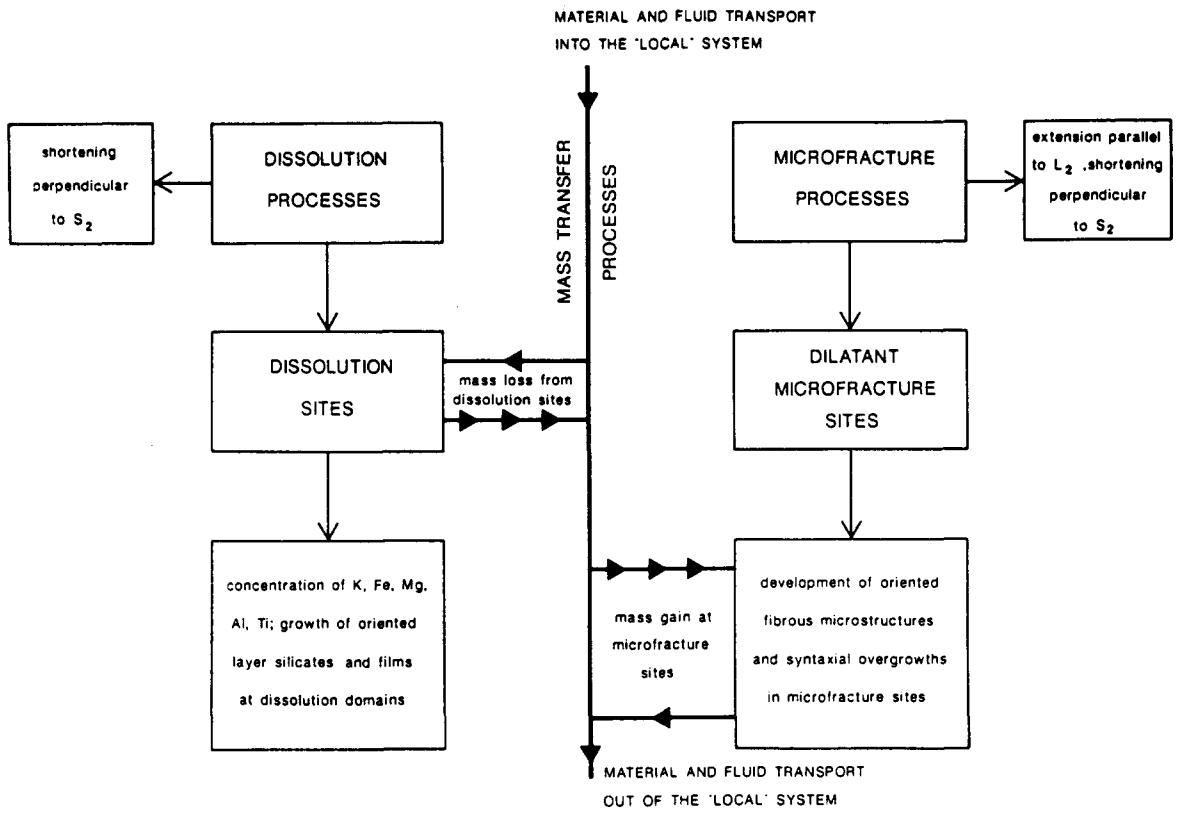

Fig. 9. Summary diagram illustrating the sequence of processes involved in the development of deformation microfabrics during the dissolution–precipitation creep process.

modated shortening at high angles to the mesoscopic foliation (Fig. 9). The repeated opening and sealing of grain-scale extension microfractures in the interfilm domains has resulted in local volume increase by extension subparallel to the mesoscopic lineation. Less significant displacement or grain translation associated with the development of oblique extension and compressive shear microfractures has accommodated shortening at high angles to the foliation, as well as elongation subparallel to the lineation. For strain compatibility to be maintained at the boundaries between film and interfilm domains, film growth must also have involved a component of extension parallel to the lineation direction.

Fibrous microstructures in extension microfracture sites have been shown to be straight to gently curved, with fibre axes subparallel to the total extension direction across microfractures, regardless of the orientation of microfracture walls. Importantly, the face-controlled fringe structures around pyrite euhedra are also typically nearly straight, and indicate that microfracture dilatancy has been generated by coaxial extension subparallel to the L_2 lineation.

Shortening within interfilm domains has generally been minimal, with most of the bulk-rock shortening being accommodated by volume loss from film domains. On this basis we can make some useful observations on volume changes and strain magnitudes within the film and interfilm domains, and on the mass balance during material transfer from dissolution sites to microfracture sites. Comparison of typical bulk strains (see section on Geological Setting) with typical relative volume fractions occupied by film domains and interfilm domains (Fig. 10), indicates that volume loss from dissolution zones has been of a similar magnitude to volume increase associated with mineral growth in dilatant microfractures within the interfilm domains. In the model illustrated in Fig. 10 an overall bulk shortening of 50% has been accommodated by plane strain shortening of about 90% normal to the foliation in film and film-cluster domains. This requires a volume loss of around 70% within the film domains and corresponds to dissolution of about 50% of the total rock volume. In the interfilm domains, negligible shortening normal to S_2, but extension of about 100% parallel to L_2 results in a volume increase comparable with the volume loss from adjacent dissolution zones.

We have seen that Si has been the dominant component removed from dissolution sites. The high abundance of quartz relative to layer silicates in microfracture sites in a number of examples is consistent with essentially conservative mass transfer from dissolution sites to adjacent microfracture sites. Nevertheless, there is a significant number of cases in which layer silicates are the dominant phase filling microfracture sites despite the bulk rock composition being dominated by quartz and feldspar. Such an imbalance between the chemistry of adjacent material sources and sinks indicates that the size of the closed system during solution–precipitation creep can be somewhat larger than the separation of adjacent material sources and sinks.

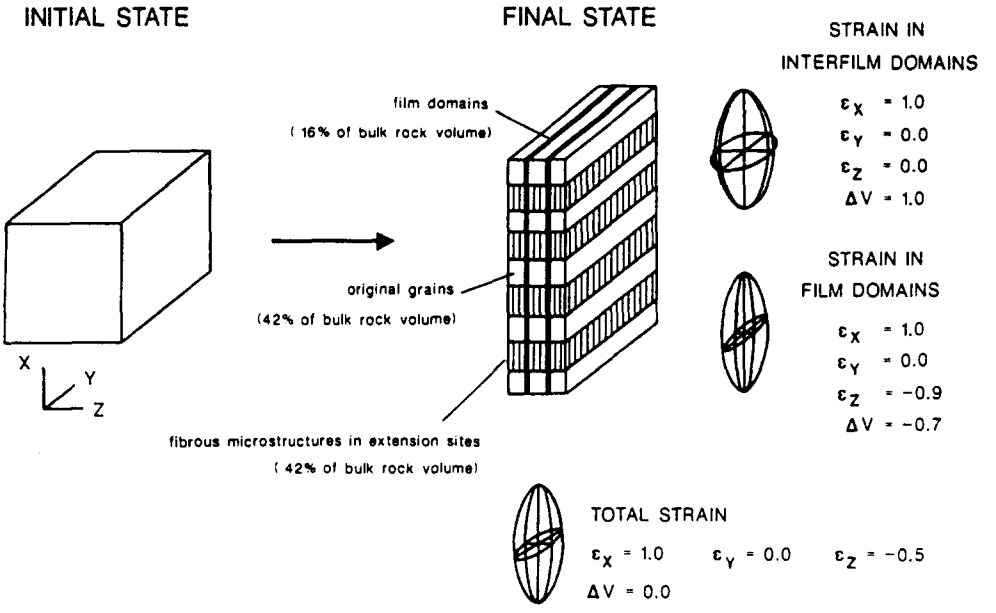

Fig. 10. Schematic illustration of typical approximate strain distribution and volume changes in film and interfilm domains. For typical strains ($\varepsilon_z = -0.5$, $\varepsilon_y = 0.0$, $\varepsilon_x = 1.0$), the usual volume proportions of primary (pre-deformation) fabric elements, layer silicate film domains and fibrous microstructures in extension sites in interfilm domains, suggest that in many cases volume loss at dissolution sites has been approximately balanced by volume increase at microfracture sites.

Dissolution, solution transfer and precipitation processes

The microstructural evidence overwhelmingly indicates that aqueous fluids in an extensive grain boundary and microcrack network have played a major role in controlling deformation and mass transfer processes during cleavage development in the Mount Lyell area. TEM indicates the ubiquitous presence of bubbles on grain boundaries and along sealed microfractures, particularly in quartz and feldspar. Bubbles on healed microfracture surfaces are clearly the necked-down remnants of originally more continuous fluid films (Roedder 1981). Abundant bubbles found on grain boundaries are the remnants of micropores or originally continuous thin fluid films (White & White 1981, Urai *et al.* 1986).

Any general solution–precipitation creep model which can explain the formation of deformation microfabrics of the type that we have described must involve a series of steps as follows:

(1) dissolution of minerals at particular sites;
(2) transport of dissolved species either by diffusion through a standing fluid, or by transport in a migrating fluid;
(3) nucleation and growth of minerals from solution at particular sites.

A number of models have previously been proposed as controlling dissolution–precipitation creep processes in non-hydrostatically stressed grain aggregates. The usual models involve dissolution at solution–solid interfaces with high normal stress (e.g. Durney 1972, 1976, 1978, Paterson 1973, Rutter 1976, Robin 1978, 1979, Raj 1982, Green 1984). Many of these models assume a closed system in which the solid is stressed by a permeable loading frame and is in contact with a fluid at uniform pressure. Local dissolution and diffusive mass transfer occur in response to stress-generated chemical potential gradients around solution–solid interfaces. Precipitation and mineral growth are envisaged to occur preferentially at interfaces having relatively low normal stress.

Such models are an oversimplification of geological situations such as that illustrated in this paper. In particular, orientation-dependent dissolution may be influenced by a number of factors other than variations in chemical potential due to changes in normal stress and elastic strain energy around grains. The operation of microcrack sealing processes in competition with grain-scale microcrack growth may be expected to result in transient connectivity between elements of the fluid-filled grain boundary and microcrack network. In such circumstances, temporarily isolated fluid-containing

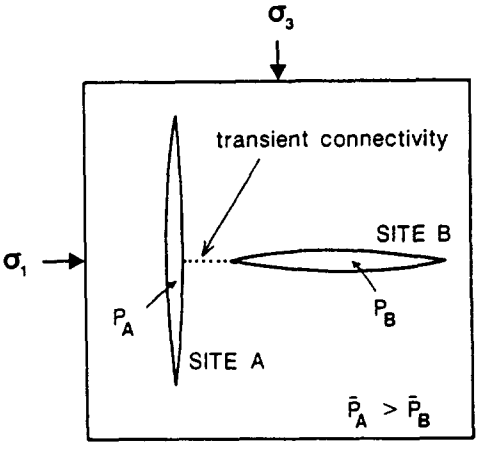

Fig. 11. Transient connectivity between elements of the fluid-containing network may result in time-statistical variations in fluid pressure between fluid films or microcracks (A) inclined at high angles to σ_1 and dilatant microcracks (B) oriented at high angles to σ_3. If average fluid pressure, P_A, in site A is higher than the average fluid pressure, P_B in site B, then the usual pressure dependence of mineral solubilities will tend to result in mass transfer from A to B.

boundaries or microcracks which are oriented at high angles to the local maximum principal stress may develop fluid pressures which are higher than those in dilating microcracks oriented at low angles to the local maximum principal stress (Fig. 11). The positive pressure dependence of the solubilities of many minerals (Fournier & Potter 1982, Helgeson & Lichtner 1987) means that microstructural sites which time-statistically have higher than average fluid pressures may preferentially evolve as dissolution sites, whereas microstructural sites such as dilatant microfractures having lower time-averaged fluid pressures will evolve as precipitation sites.

The distribution and physical structure of the fluid phase in rocks deforming by solution–precipitation creep may also be of fundamental importance in controlling the dissolution–precipitation geometry. In dilatant microcracks, the fluid phase will have properties approaching that of bulk fluid. However, Rutter (1976, 1983) and Fyfe *et al.* (1978) have argued that any aqueous fluid distributed along grain boundaries in metamorphic rocks will typically occur as thin films. Such aqueous films adsorbed onto boundaries are unlikely to have the same physical structure and thermodynamic properties as bulk water (Drost-Hansen 1969). Thus we do not expect the solubilities and dissolution rate laws for minerals in thin fluid films to be the same as those pertaining in a bulk-fluid phase such as would exist in a dilatant microcrack. Indeed, Rutter (1983) has suggested that solute concentrations in thin aqueous films are likely to be *higher* than in bulk water. If this is the case, then concentration gradients between thin films (along grain boundaries having high normal stress) and 'bulk'-fluid sites such as dilatant microcracks, could be of major significance in controlling the geometry of mass transfer during solution–precipitation creep.

Many solution–precipitation creep models have involved mass transfer purely by grain-scale solute diffusion down stress-controlled chemical potential gradients. Somewhat more local diffusion driven by surface energy effects may also influence the healing of narrow fluid-filled microcracks (Smith & Evans 1984). However, diffusional transport processes need not control the rate at which material is transported to, and deposited within dilatant microcrack sites. Increasing evidence that mass transfer during cleavage development can involve path lengths much larger than can be reasonably achieved by diffusional transport, and certainly larger than the shortest paths of high, stress-induced chemical potential gradients (Wright & Platt 1982, Etheridge *et al.* 1983, 1984) requires that fluid migration plays a major role in facilitating mass transport in some environments. We earlier argued that transient differences in fluid pressure between various parts of the fluid-containing grain-boundary and microcrack network are likely when grain-scale dilatancy is an integral part of the deformation process. Under these circumstances, dilatancy-driven fluid pumping (Etheridge *et al.* 1984, Lister *et al.* 1986) is likely to influence mass transport rates by cycling fluid between grain-boundary fluid films and dilating microcracks. It is important to emphasize, however, that there may be significant transient variations in fluid pressures not just between adjacent microstructural sites, but also between different parts of a deforming rock mass.

Transient fluid pressure variations on scales much larger than grain size can arise as a consequence of mechanical and stress heterogeneity causing unusually large cyclic dilatancy variations in particular structural sites. The dilatant fault jogs of Sibson (1985) are spectacular examples of such structurally induced variations in dilatancy, which thereby control fluid migration. We suggest that this concept should be extended to the more subtle variations in stress and strain rate, and therefore dilatancy, which will occur in most deforming rock masses. The geometry of mass transfer and the separation of material sources and sinks in such situations will be influenced by factors such as fluid chemistry, host-rock mineralogy, and the P–T path of the migrating fluid during the dilatancy pumping cycle. Repeated fluid cycling between grain-boundary fluid networks and dilatant structural sites has the potential to generate high effective fluid–rock ratios and result in major large-scale mass transfer via migrating fluids. Importantly, the macroscopic variations in dilatancy can readily drive fluids laterally or even downwards in overpressured rock masses, giving rise to effective fluid recirculation.

In fluid-dominated deformation regimes where rocks are potentially chemically open systems on large scales, the overall strain pattern and any attendant volume changes will clearly be dependent on competition between volume loss at dissolution sites and volume gain at nearby microfracture sites. It is expected that in general there can be domains having substantial volume loss or volume gain, as well as domains in which volume has been conserved during foliation development. Recognition of the distance scales on which mass transfer has occurred, as well as the distribution of domains of bulk volume loss and volume gain are potentially powerful tools for the analysis of both fluid migration patterns and processes driving fluid migration during regional deformation and metamorphism.

The role of high-pressure fluids in controlling mechanical behaviour during cleavage development: implications for crustal rheology

The volcanic sequence at Mount Lyell was deformed at temperatures around 300°C and at lithostatic pressures between about 200 and 300 MPa (Cox 1981). Current models for the depth-dependent rheology of the continental crust suggest that crustal strengths are near maximum under such conditions (Meissner & Strehlau 1982, Sibson 1983, Carter & Tsenn 1987) (Fig. 12a). These models are based on the assumption that only two deformation mechanisms, macroscopic frictional sliding and dislocation creep, control crustal strength. They predict that strength will be at a maximum near the transition between these mechanisms (usually referred to as the brittle–ductile transition), and generally ignore

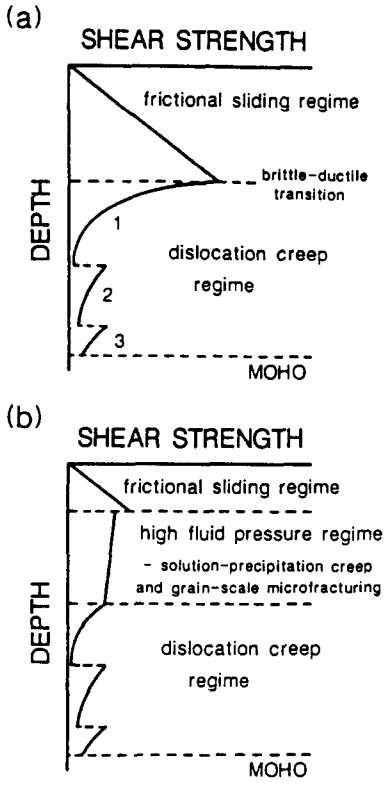

Fig. 12. (a) Schematic shear strength vs depth profile typical of many depth-dependent rheological models for the continental crust. The models assume that upper crustal strength is controlled by a friction relation of the type described by Byerlee (1978), and that the strength of the lower part of the continental crust is controlled by dislocation flow processes. Illustrated are schematic power-law relations for (1) quartz-rich rock types, (2) feldspar-dominated rocks and (3) mafic rocks. A major continental 'stress guide' (Lister & Davis 1989) is defined by the region of high strength at around the depth of the 'brittle–ductile transition' zone. (b) Schematic depth-dependent rheological model in which the operation of solution-precipitation creep processes, coupled with grain-scale dilatancy at high fluid pressures, dramatically reduces mid- to upper-crustal strengths, thereby removing the major continental stress guide and leading to major crustal deformation.

or minimize the role of the fluid-phase in controlling the deformation process.

The microstructures and deformation processes described in this paper have a number of implications for crustal rheology which are at variance with conventional depth-dependent rheological models which are based entirely on laboratory experiments.

(1) The abundant microscopic to mesoscopic extension veins, which have formed during cleavage development at Mount Lyell indicate that near-lithostatic fluid pressures, and thus low effective confining pressures, have been maintained during a substantial part of the deformation history (Secor 1968, Phillips 1972). Laboratory studies have demonstrated the importance of microcracking and attendant dilatancy as a major deformation mechanism at low effective confining pressures (Handin *et al.* 1963, Edmond & Paterson 1972, Zoback & Byerlee 1975, Fischer & Paterson in press). Indeed Rutter *et al.* (1985) have not only demonstrated experimentally that intergranular dilatation is important at elevated fluid pressures, but have also produced intergranular fibrous microstructures very similar to those we have described. Thus, the importance of repeated grain-scale microfracturing such as we have described is seen to be a direct consequence of high fluid pressures prevailing during cleavage development.

(2) The ubiquitous evidence for repeated extension fracturing at a wide range of scales limits stress differences at the time of fracture to a few tens of megapascals (Etheridge 1983). Thus, despite the importance of microfracturing as a deformation mechanism, the rock strength and deformation processes during cleavage development are clearly not described by frictional behaviour (e.g. Byerlee 1978). The low inferred strength during coupled solution–precipitation creep and grain-scale fracturing at high fluid pressures is in marked contrast to the much higher, essentially strain-rate independent strengths typical during pervasive cataclastic deformation of most crustal materials tested at low to moderate temperatures and elevated effective confining pressures (Paterson 1978). We are led to the conclusion then, that the development of near-lithostatic fluid pressures, and consequent enhancement of microfracture and grain translation processes in conjunction with solution–precipitation creep, must have a dramatic effect in reducing upper crustal strengths to levels well below those inferred for low fluid pressure, or essentially non-metamorphic environments.

(3) The major deformation processes that we have described (extension microfracture, dissolution–precipitation and mass transport in a fluid phase) are predicted to have flow laws which are less sensitive to both stress and temperature than is the case for processes such as dislocation creep (Raj 1982, Rutter 1983, Etheridge *et al.* 1984). This can be particularly so if mass transport via a mobile fluid phase is deformation rate controlling (Etheridge *et al.* 1984). The occurrence of solution-transfer processes in nature over a large temperature range (Rutter 1983) supports the concept of low temperature sensitivity.

Even though the microstructures described in this paper are spectacular examples of their type, features such as these are very widespread in low to medium-grade metamorphic rocks (see Etheridge *et al.* 1984 and Cox *et al.* 1987 for reviews). We therefore suggest that the rheology of the upper to middle crust *during deformation under prograde metamorphic conditions* may not be adequately described by the conventional depth-dependent rheology models (Fig. 12a). Rather, substantial regions in the crust may have flow behaviour characterized by relatively low strength and low stress and temperature sensitivities.

The qualitative effect of adding such deformation behaviour to depth-dependent rheological models is illustrated in Fig. 12(b). The low 'yield stress' indicated by ubiquitous extension fracturing raises the 'brittle–ductile' transition, and together with the low temperature-dependence of flow strength, gives rise to a much more uniform strength with depth. We have assumed in Fig. 12(b) that dislocation creep becomes strength controlling in the mid- to lower-crust. It must be emphasized

that there is no implicit suggestion that the crustal rheology represented by Fig. 12(b) applies to all crustal and tectonic settings. Rather, it is considered to be mainly restricted to active 'mobile belts' during prograde regional metamorphism.

CONCLUSIONS

The microstructures associated with cleavage development in the volcanic rocks of the Mount Lyell area illustrate the importance of high fluid pressures in controlling deformation mechanisms and crustal strengths. Under the ambient low-grade metamorphic conditions, dissolution–precipitation processes have operated together with grain-scale microfracture processes. The demonstration of the importance of grain-scale dilatancy during deformation is significant in that it indicates that deformation has occurred at low stress differences and low effective stresses, with a discrete high-pressure fluid-phase occupying a grain-scale network. Fibrous microstructures developed by crack–seal mechanisms in dilatant microcracks form a very significant component of the foliation/lineation defining fabric elements.

A number of processes have been proposed as possibly influencing the geometry of dissolution–precipitation creep. These include material transfer in response to stress-controlled variations in chemical potential around non-hydrostatically stressed grains. However other factors, such as time-statistical variations in fluid pressure between dissolution sites and microfracture sites, as well as variations in mineral solubility between thin, grain-boundary fluid films and fluid-filled microcracks, may also have important effects.

Mass transfer between material sources and sinks may have occurred by solute diffusion through an essentially static fluid network and/or by transport with a migrating fluid. Grain-scale dilatancy-driven fluid pumping in response to transient fluid pressure variations between elements of the fluid-containing network is likely to have been particularly important. Mass transfer over significantly larger distances can have been facilitated by fluid pumping between grain-scale fluid networks and particular macrostructural sites having cyclic dilatancy. Mismatches between the chemistry of adjacent material sources and sinks indicate that the true separation of sources and sinks probably has been somewhat larger than grain size. Thus fluid migration has probably played a major role in controlling material transfer during cleavage development.

The operation of grain-scale microfracture and mass-transfer processes as dominant deformation mechanisms at high fluid pressures is expected to lead to high fluid pressure crustal regimes becoming substantially weaker than low fluid pressure crustal regimes. Such weakening in mid- to upper-crustal environments may be a significant factor triggering major regional deformation episodes.

Acknowledgements—This study has been financially supported by an Australian Government Postgraduate Research Award and a Queen Elizabeth II Research Fellowship held by one of us (S.F.Cox) at Monash University. We are grateful to the Mount Lyell Mining and Railway Co. Ltd for ready access to their lease area, and for support in the field. Philip Stevens, of the B.H.P. Melbourne Research Laboratories, kindly provided assistance with X-ray fabric facilities. George Fischer, Bruce Hobbs, Gordon Lister and Mervyn Paterson are all thanked for stimulating discussion during various stages of the study.

REFERENCES

Alvarez, W., Engelder, T. & Geiser, P. 1978. Classification of solution cleavage in pelagic limestones. *Geology* **6**, 263–266.

Beach, A. 1974. A geochemical investigation of pressure solution and the formation of veins in a deformed greywacke. *Contr. Miner. Petrol.* **46**, 61–68.

Beutner, E. C. & Charles, E. G. 1985. Large volume loss during cleavage formation, Hamburg sequence, Pennsylvania. *Geology* **13**, 803–805.

Borradaile, G. J. 1981. Particulate flow of rock and the formation of cleavage. *Tectonophysics* **72**, 305–321.

Borradaile, G. J., Bayly, M. B. & Powell, C. McA. (eds) 1982. *Atlas of Deformational and Metamorphic Rock Fabrics*. Springer-Verlag, Berlin.

Byerlee, J. D. 1978. Friction of rocks. *Pure & Appl. Geophys.* **116**, 615–626.

Carter, N. L. & Tsenn, M. C. 1987. Flow properties of continental lithosphere. *Tectonophysics* **136**, 27–63.

Corbett, K. D. 1981. Stratigraphy and mineralization in the Mt Read Volcanics, Western Tasmania. *Econ. Geol.* **76**, 209–230.

Cox, S. F. 1981. The stratigraphic and structural setting of the Mt Lyell volcanic-hosted sulfide deposits. *Econ. Geol.* **76**, 231–245.

Cox, S. F. & Etheridge, M. A. 1983. Crack–seal fibre growth mechanisms and their significance in the development of oriented layer silicate microstructures. *Tectonophysics* **92**, 147–170.

Cox, S. F., Etheridge, M. A. & Wall, V. J. 1987. The role of fluids in syntectonic mass transport, and the localization of metamorphic vein-type ore deposits. *Ore Geology Rev.* **2**, 65–86.

Drost-Hansen, W. 1969. On the structure of water near solid interfaces, and the possible existence of long range order. *Ind. & Engng Chem.* **61**, 10–47.

Durney, D. W. 1972. Solution-transfer, an important geological deformation mechanism. *Nature* **235**, 315–317.

Durney, D. W. 1976. Pressure solution and crystallization deformation. *Phil. Trans. R. Soc. Lond.* **A283**, 229–240.

Durney, D. W. 1978. Early theories and hypotheses on pressure-solution–redeposition. *Geology* **6**, 369–372.

Durney, D. W. & Ramsay, J. G. 1973. Incremental strains measured by syntectonic crystal growth. In: *Gravity and Tectonics* (edited by De Jong, K. A. & Scholten, R.). Wiley, New York, 67–69.

Edmond, J. M. & Paterson, M. S. 1972. Volume changes during deformation of rocks at high pressures. *Int. J. Rock Mech. Min. Sci.* **9**, 161–192.

Engelder, T. 1984. The role of pore water circulation during the deformation of foreland fold and thrust belts. *J. geophys. Res.* **89**, 4319–4325.

Etchecopar, A. & Malavieille, J. 1987. Computer models of pressure shadows: a method for strain measurement and shear sense determination. *J. Struct. Geol.* **9**, 667–677.

Etheridge, M. A. 1983. Differential stress magnitudes during regional deformation and metamorphism–upper bound imposed by tensile fracturing., *Geology* **11**, 231–234.

Etheridge, M. A., Wall, V. J. & Vernon, R. H. 1983. The role of the fluid phase during regional deformation and metamorphism. *J. Metam. Geol.* **1**, 205–226.

Etheridge, M. A., Wall, V. J., Cox, S. F. & Vernon, R. H. 1984. High fluid pressures during regional metamorphism and deformation: implications for mass transport and deformation mechanisms. *J. geophys. Res.* **89**, 4344–4358.

Fischer, G. J. & Paterson, M. S. In press. Dilatancy during rock deformation at high temperatures and pressures. *J. geophys. Res.*

Fourner, R. O. & Potter, R. W. II. 1982. An equation correlating the solubility of quartz in water from 25°C to 900°C at pressures up to 10,000 bars. *Geochim. cosmochim. Acta* **46**, 1969–1973.

Fyfe, W. S., Price, N. J. & Thompson, A. B. 1978. *Fluids in the Earth's Crust*. Elsevier, Amsterdam.

Geiser, P. A. & Sansone, S. 1981. Joints, microfractures and the formation of solution cleavage in limestone. *Geology* **9**, 280–285.

Gratier, J. P. 1983. Estimation of volume changes by comparative chemical analyses in heterogeneously deformed rocks (folds with mass transfer). *J. Struct. Geol.* **5**, 329–339.

Gray, D. R. 1978. Cleavages in deformed psammitic rocks from southeastern Australia: Their nature and origin. *Bull. geol. Soc. Am.* **89**, 577–590.

Green, H. W. 1984. "Pressure solution" creep: some causes and mechanisms. *J. geophys. Res.* **89**, 4313–4318.

Gregg, W. J. 1985. Microscopic deformation mechanisms associated with mica film formation in cleaved psammitic rocks. *J. Struct. Geol.* **7**, 45–56.

Handin, J., Hager, R. V., Friedman, M. & Feather, J. N. 1963. Experimental deformation of sedimentary rocks under confining pressure: pore pressure tests. *Bull. Am. Ass. Petrol. Geol.* **47**, 717–755.

Helgeson, H. C. & Lichtner, P. C. 1987. Fluid flow and mineral reactions at high temperatures and pressures. *J. geol. Soc. Lond.* **144**, 313–326.

Kerrich, R. 1978. An historical review and synthesis of research on pressure solution. *Zentbl. Miner. Geol. Paläont.* **5/6**, 512–550.

Lister, G. S., Boland, J. N. & Zwart, H. J. 1986. Step-wise growth of biotite porphyroblasts in pelitic schists of the western Lys-Caillaouas massif (Pyrenees). *J. Struct. Geol.* **8**, 543–562.

Lister, G. S. & Davis, G. A. 1989. The origin of metamorphic core complexes and detachment faults formed during Tertiary continental extension in the northern Colorado River region, U.S.A. *J. Struct. Geol.* **11**, 65–94.

Means, W. D. 1975. Natural and experimental microstructures in deformed micaceous sandstone. *Bull. geol. Soc. Am.* **86**, 1221–1229.

Means, W. D. 1977a. Experimental contributions to the study of foliations in rocks: a review of research since 1960. *Tectonophysics* **39**, 329–354.

Means, W. D. 1977b. A deformation experiment in transmitted light. *Earth Planet. Sci. Lett.* **35**, 169–179.

Meissner, R. & Strehlau, J. 1982. Limits of stresses in continental crust and their relationship to depth-frequency distribution of shallow earthquakes. *Tectonics* **1**, 73–89.

Nickelsen, R. P. 1972. Attributes of rock cleavage in some mudstones and limestones of the Valley and Ridge Province, Pennsylvania. *Penn. Acad. Sci. Proc.* **46**, 107–112.

Paterson, M. S. 1973. Non-hydrostatic thermodynamics and its geological applications. *Rev. Geophys. & Space Phys.* **11**, 355–390.

Paterson, M. S. 1978. *Experimental Rock Deformation: The Brittle Field.* Springer-Verlag, Berlin.

Phillips, W. J. 1972. Hydraulic fracturing and mineralization. *J. geol. Soc. Lond.* **128**, 337–359.

Raj, R. 1982. Creep in polycrystalline aggregates by matter transport through a liquid phase. *J. geophys. Res.* **87**, 4731–4739.

Ramsay, J. G. 1980. The crack-seal mechanism of rock deformation. *Nature* **284**, 135–139.

Ramsay, J. G. & Huber, M. 1983. *The Techniques of Modern Structural Geology. Volume I: Strain Analysis.* Academic Press, London.

Reid, K. O. 1975. Mt Lyell copper deposits. In: *Economic Geology of Australia and Papua-New Guinea, I. Metals* (edited by Knight, C. L.). *Aust. Inst. Min. Metal. Monogr.* **5**, 604–619.

Robin, P.-Y. F. 1978. Pressure solution at grain-to-grain contacts. *Geochim. cosmochim. Acta* **42**, 1383–1389.

Robin, P.-Y. F. 1979. Theory of metamorphic segregation and related processes. *Geochim. cosmochim. Acta* **43**, 1587–1600.

Roedder, E. 1981. Origin of fluid inclusions and changes that occur after trapping. In: *Fluid Inclusions—Applications to Petrology* (edited by Hollister, L. S. & Crawford, M. L.). *Mineral Assoc. Can. Short Course Notes* **6**, 101–137.

Rutter, E. H. 1976. The kinetics of rock deformation by pressure solution. *Phil. Trans. R. Soc. Lond.* **A283**, 203–219.

Rutter, E. H. 1983. Pressure solution in nature, theory and experiment. *J. geol. Soc. Lond.* **140**, 725–740.

Rutter, E. H., Peach, C. J., White, S. H. & Johnston, C. 1985. Experimental 'syntectonic' hydration of basalt. *J. Struct. Geol.* **7**, 251–256.

Secor, D. T. 1968. Mechanics of natural extension fracturing at depth in the Earth's crust. *Geol. Surv. Canada Pap.* 68–52, 3–48.

Sibson, R. H. 1983. Continental fault structure and the shallow earthquake source. *J. geol. Soc. Lond.* **140**, 741–767.

Sibson, R. H. 1985. Stopping of earthquake ruptures at dilational fault jogs. *Nature* **316**, 248–251.

Simmons, G. & Richter, D. 1976. Microcracks in rocks. In: *The Physics and Chemistry of Minerals and Rocks* (edited by Strens, R. C. J.). Wiley and Sons, London, 105–137.

Smith, D. L. & Evans, B. 1984. Diffusional crack healing in quartz. *J. geophys. Res.* **89**, 4125–4136.

Southwick, D. L. 1987. Bundled slaty cleavage in laminated argillite, north-central Minnesota. *J. Struct. Geol.* **9**, 985–993.

Urai, J., Means, W. D. & Lister, G. S. 1986. Dynamic recrystallization of minerals. In: *Mineral and Rock Deformation: Laboratory Studies—The Paterson Volume* (edited by B. E. Hobbs & H. C. Heard). *Am. Geophys. Un. Geophys. Monogr.*, **36**, 161–199.

White, J. & White, S. H. 1981. On the structure of grain boundaries in tectonites. *Tectonophysics* **78**, 613–628.

Williams, E. 1978. Tasman Fold Belt system in Tasmania. *Tectonophysics* **48**, 159–205.

Williams, P. F. 1972a. Development of metamorphic layering and cleavage in low grade metamorphic rocks at Bermagui, Australia. *Am. J. Sci.* **272**, 1–47.

Williams, P. F. 1972b. "Pressure shadow" structures in foliated rocks from Bermagui, New South Wales, *J. geol. Soc. Aust.* **18**, 371–377.

Wright, T. O. & Platt, L. B. 1982. Pressure dissolution and cleavage in the Martinsburg Shale. *Am. J. Sci.* **282**, 122–135.

Zoback, M. D. & Byerlee, J. D. 1975. Permeability and effective stress. *Bull. Am. Ass. Petrol. Geol.* **59**, 154–158.